An automatic tool for thoracic aorta segmentation and 3D geometric analysis

Degree of Doctor in Philosophy in
Computational Mechanics and Advanced Materials
at Istituto Universitario degli Studi Superiori di Pavia, Italy


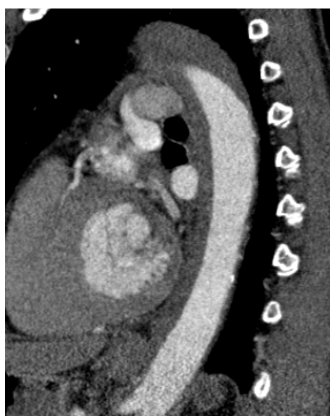

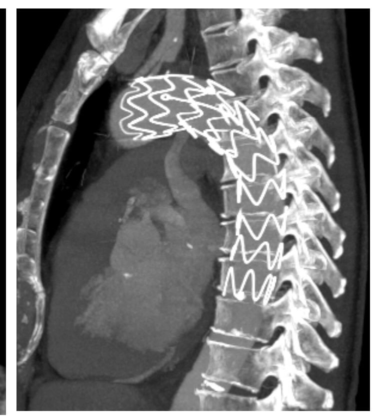


PhD candidate: Chiara Trentin

January 19, 2016, Pavia, Italy

Introduction

The aorta

- **main artery** of the human body, it carries oxygenated blood to all parts of the body
- common pathology of the thoracic aorta are: **thoracic aortic aneurysm** (TAA) and **thoracic aortic dissection of type B** (TBAD)
- deformation of the vessel with risk of **rupture**

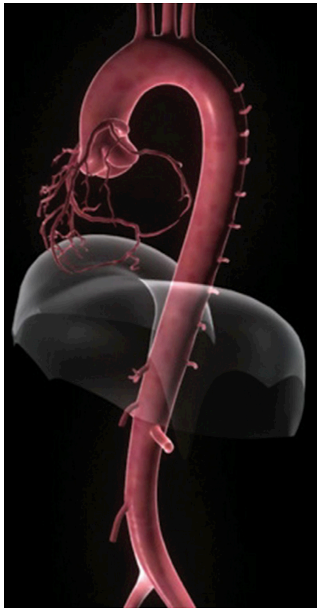
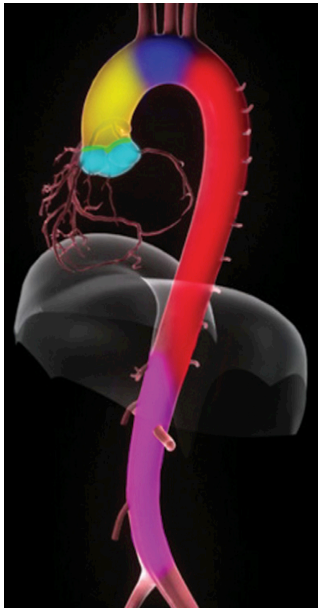
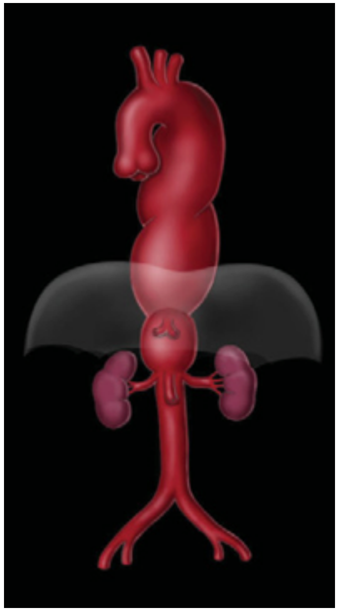
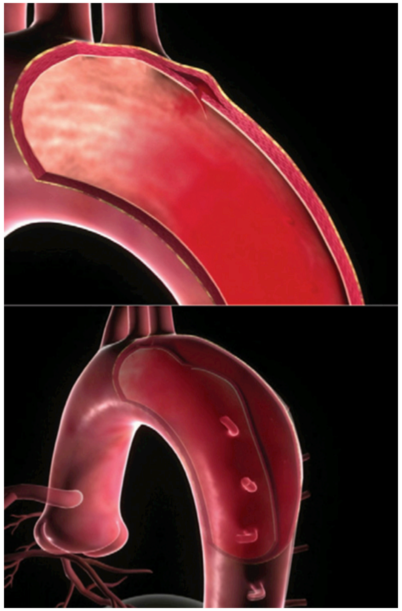

Surgical treatment

- treated with **endovascular** technique: thoracic endovascular aortic repair (**TEVAR**)
- the procedure involves the placement of an expandable **stent-graft:** metallic mesh covered with a dacron skirt
- no need of open surgery
- TEVAR for TBAD is **increasing** rapidly

Introduction

Background

- the thoracic aorta is a **pulsatile environment** and experiences high hemodynamic forces

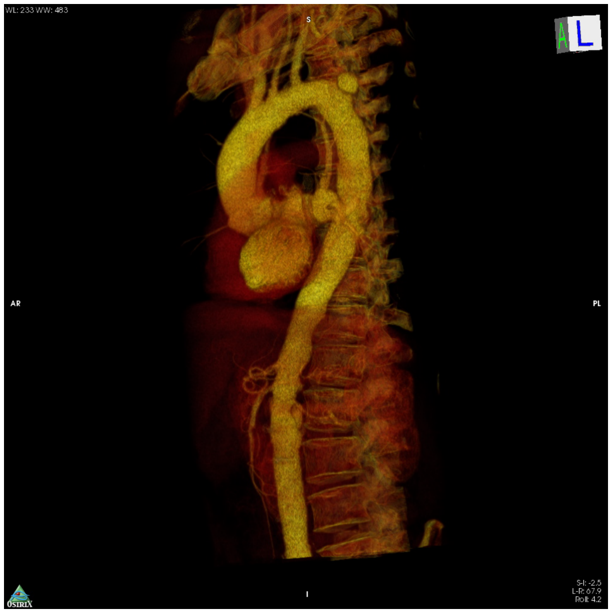

ECG-Gated CTA w\o stent

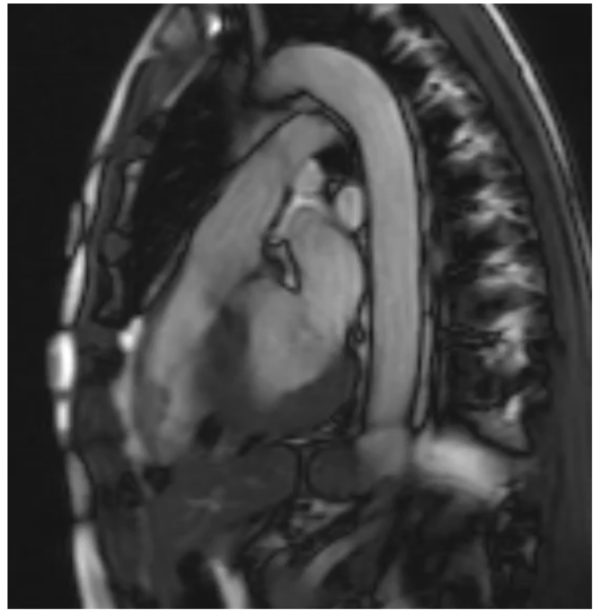

ECG-Gated CTA w\o stent

ECG-Gated CTA w\ stent

Drawbacks

- long term durability not established yet
- side branches revascularization need to be addressed

AIMs:

- clarify the **role of stent-graft** on aortic elasticity in a pulsatile environment
- **robust, repeatable, and quantitative** analysis
- analysis of both circumferential and longitudinal aortic changes
- improve stent-graft design and durability

Tool for thoracic aortic analysis:

- set of methods, automatic
- minimum user interaction
- quantitative geometric features extraction

The tool has been **developed** exploiting Python programming language and the libraries: The Visualization Toolkit (VTK) and The Vascular Modelling Toolkit (VMTK)

State of the art

- several studies investigated the dynamic of the aorta [vanP2009] [vanK2009] [muhs2006]
- **no 3D** model segmentation
- **manual** selection of **2D** cross-sections orthogonal to the vessel
- computed only **diameter or area** changes
- found that mean diameter change is 2-20% and is preserved after TEVAR for TAA[2]

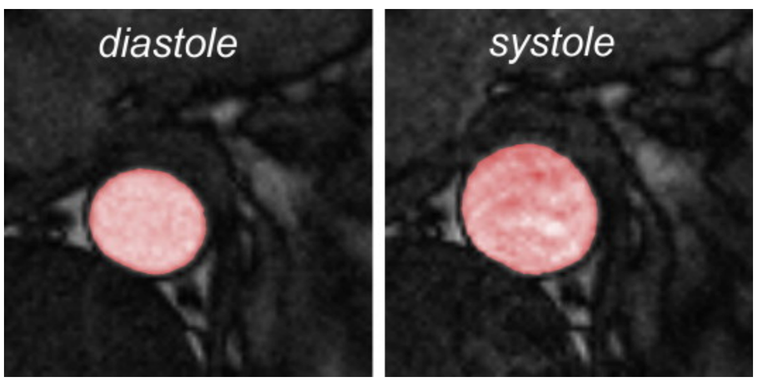

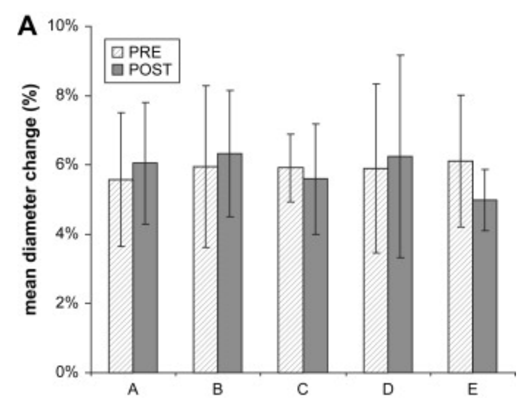

[2]van Prehn AVS 2009

The dataset

- **4D** computed tomography angiography (CTA) → images the aorta with contrast medium during **time**
- **ECG**-gated
- **8 CTA** images covering the **entire** hearth cycle
- possibility to gather **aortic dynamic changes**

ECG-Gated CTA

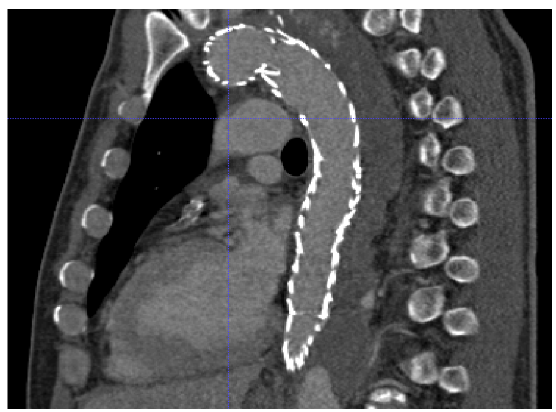

8 CTA images

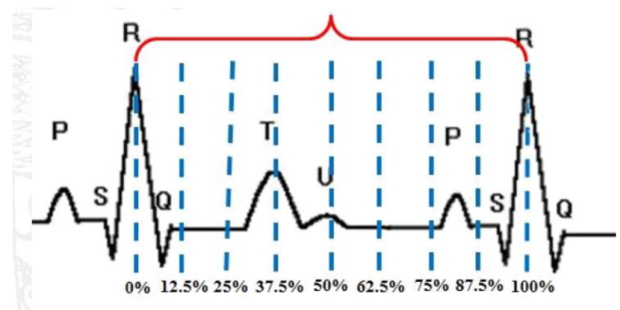

Tool outline

1. **Image pre-processing**
2. **Automatic segmentation of 4D CTA**
3. **Pre- post-TEVAR surface registration**
4. **Outer contour lines computation**
5. **Levels of interest detection**
6. **Measurements**

ECG-Gated CTA

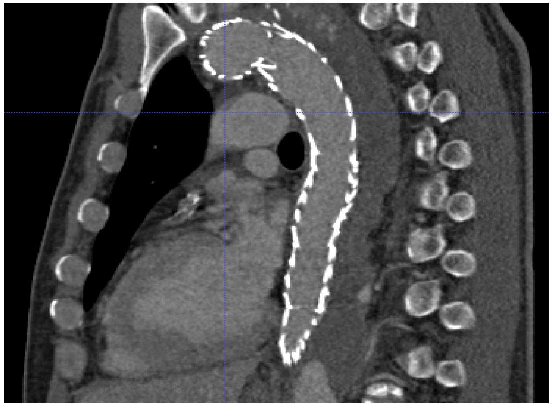

8 CTA images

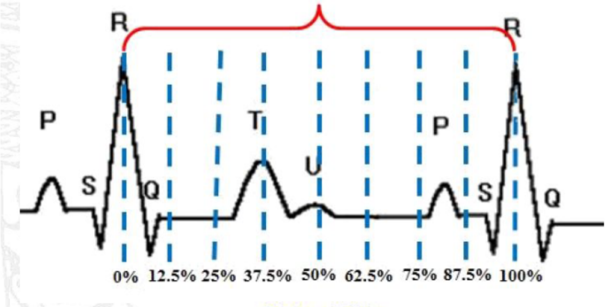

Image pre-processing

- I(**x**) is a scalar field of gray levels, with $\mathbf{x} \in \mathbb{R}^3$
- I(**x**) is composed of voxels

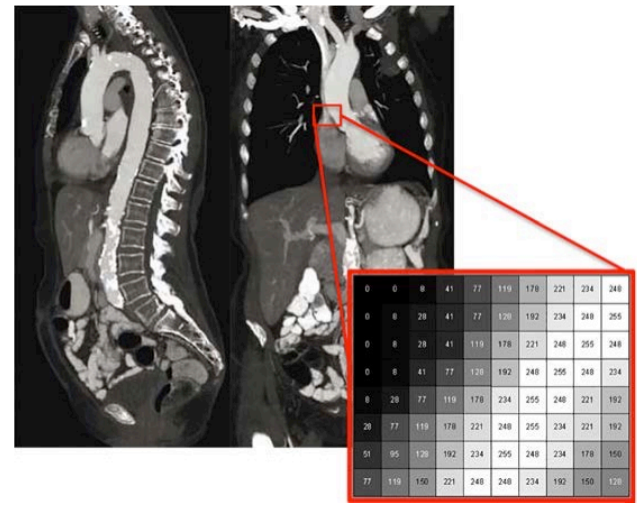

Local operator technique to suppress noise:
Image convolved with a kernel → (2k+1, 2l+1, 1)

✓ **Median filtering**

- Intensity of each Pixel_{out}: median of intensity of pixels_{in} covered by the kernel
- No edge blurring

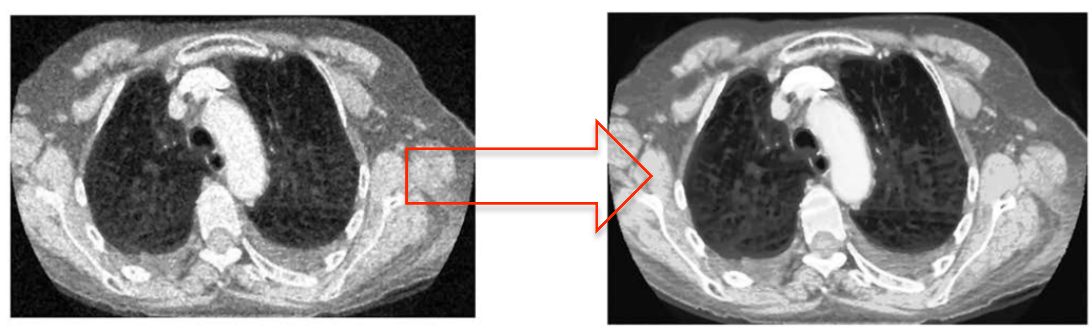

Segmentation: edge based segmentation approach is exploited

Edge detection: set of mathematical methods

Aim → identifying points at which the image brightness changes sharply

Type → search based

compute the magnitude of the image gradient and search for local directional maxima (gradient direction)

$$\nabla I = \begin{pmatrix} G_x \\ G_y \\ G_z \end{pmatrix} \begin{pmatrix} \partial I / \partial x \\ \partial I / \partial y \\ \partial I / \partial z \end{pmatrix}$$

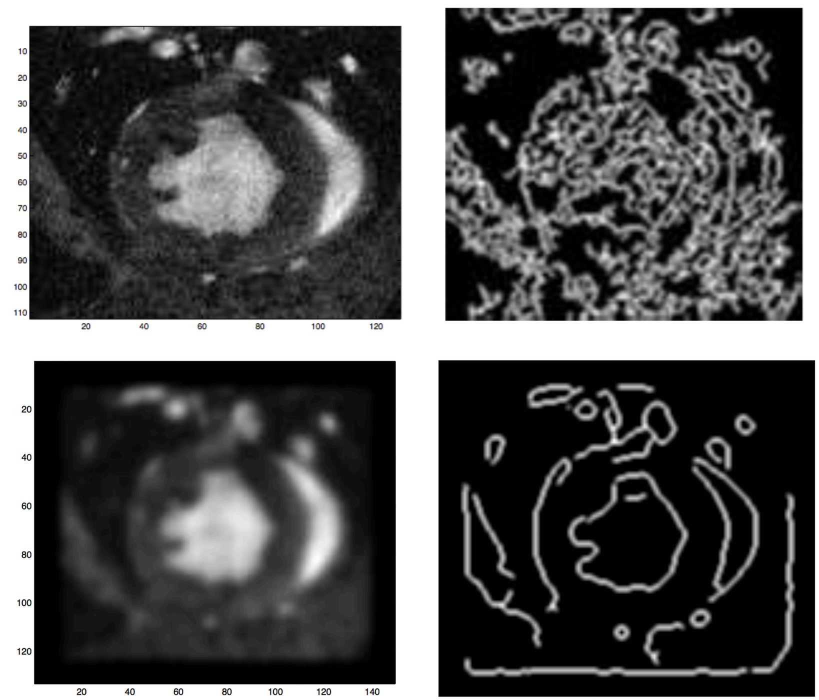

Smoothing is suggested before edge enhance

Segmentation

- based on implicit models → **level set**
- the scalar surface $S\left(\mathbf{y},t\right):\mathbb{R}^2\times\mathbb{R}^+\rightarrow\mathbb{R}^3$
- is described as a **signed distance function** $\Phi(\mathbf{x},t):\mathbb{R}^3\times\mathbb{R}^+\rightarrow\mathbb{R}$
- its **iso-surface** of level zero is the 3D model of interest $S(\mathbf{y},t)=\{\mathbf{x}|\ \Phi(\mathbf{x},t)=0\}$

Signed distance function

$$\Phi(\mathbf{x},t)=\begin{cases}-D(\mathbf{x}) & \text{if } \mathbf{x} \text{ is inside } S,\\ +D(\mathbf{x}) & \text{if } \mathbf{x} \text{ is outside } S,\\ 0 & \text{if } \mathbf{x}\in S,\end{cases}$$

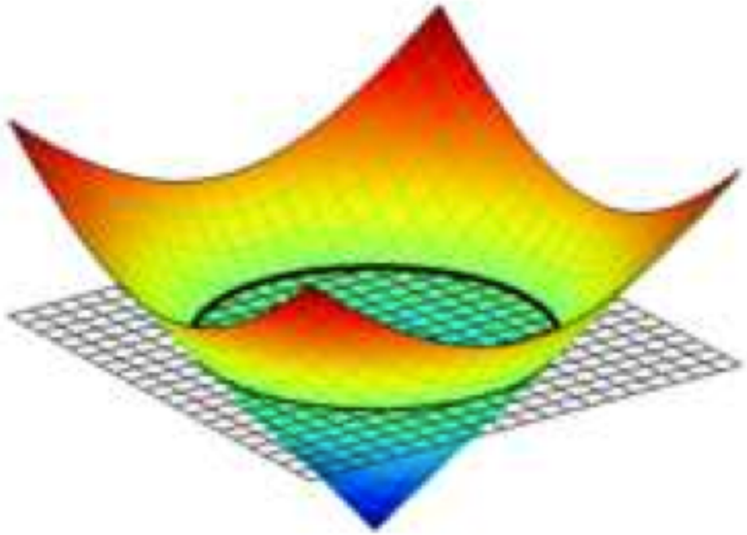

where

$$D(\mathbf{x})=\min_{\mathbf{y}\in S}\{|\ \mathbf{x}-\mathbf{y}|\ \}$$

Segmentation: 3D surface is computed solving the evolution equation in Φ [antiga2008]

$$\Phi_t = -w_1 G(\mathbf{x})\|\nabla\Phi\| + 2w_2 H(\mathbf{x})\|\nabla\Phi\| + w_3 \nabla P(\mathbf{x}) \cdot \nabla\Phi$$

where:

$G(\mathbf{x}) = \dfrac{1}{1 + \|\nabla I(\mathbf{x})\|}$	represents surface **inflation**
$H(\mathbf{x}) = \nabla \cdot \left(\dfrac{\nabla\Phi}{\|\nabla\Phi\|} \right)$	controls the **smoothness** of the surface
$P(\mathbf{x}) = -\|\nabla I(\mathbf{x})\|$	represents **advection** of the surface

weights w_1, w_2, and w_3 **guide** the influence of each term on the surface evolution

Initialization

- the level set has to be **initialized** with an initial $\Phi_0(\mathbf{x}) = \Phi(\mathbf{x}, 0)$

Automatic segmentation of 4D CTA

Segmentation: colliding front initialization[antiga2008]

- the user puts **two** seeds inside the vessel
- a **wave propagates** between the seeds and generate the initial $\phi_0(\mathbf{x})$

$$\|\nabla T_i\| = \frac{1}{1 + I(\mathbf{x})}$$

- travel time of a wave originating from a seed and traveling with velocity I(x) → faster where the image is brighter

$$\Phi_0(\mathbf{x}) = \nabla T_1 \cdot \nabla T_2$$

- negative where the two waves travel in opposite directions positive elsewhere

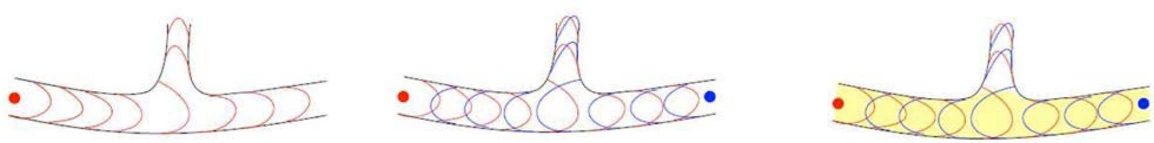

[antiga2008]

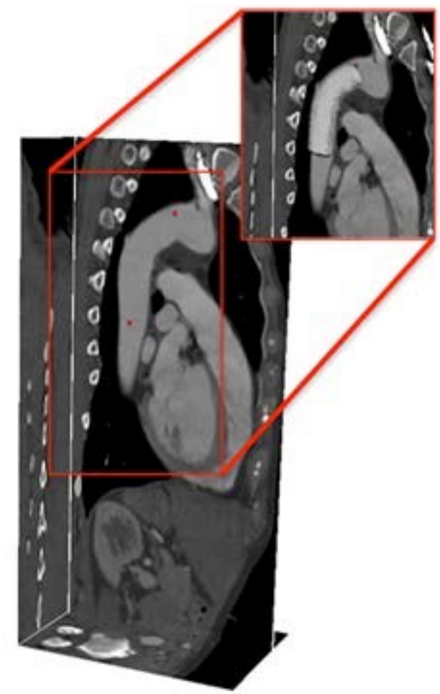

Automatic segmentation of 4D CTA[trentin2015]

- the user puts **seven** seeds inside the vessel
- **bunch of initializations** are performed looping from the first seed to the last and vice versa
- entire aorta initialized in **one shot**
- possibility to **detail** the segmentation **later**

Following function is defined and computed

$$F_k(\mathbf{x}) = \sum_{i=k}^{k+1} \sum_{j=k}^{k+1} \nabla T_i \cdot \nabla T_j, \qquad i \neq j$$

- k = 1, … , 6, i, and j represent the user defined seeds
- T_i and T_j satisfy the equation previously defined in I

We take $$\Phi_0(\mathbf{x}) = \min_{\mathbf{x} \in \mathbb{R}^3} \{F_1(\mathbf{x}), \ldots, F_6(\mathbf{x})\}$$

negative inside the vessel and positive outside

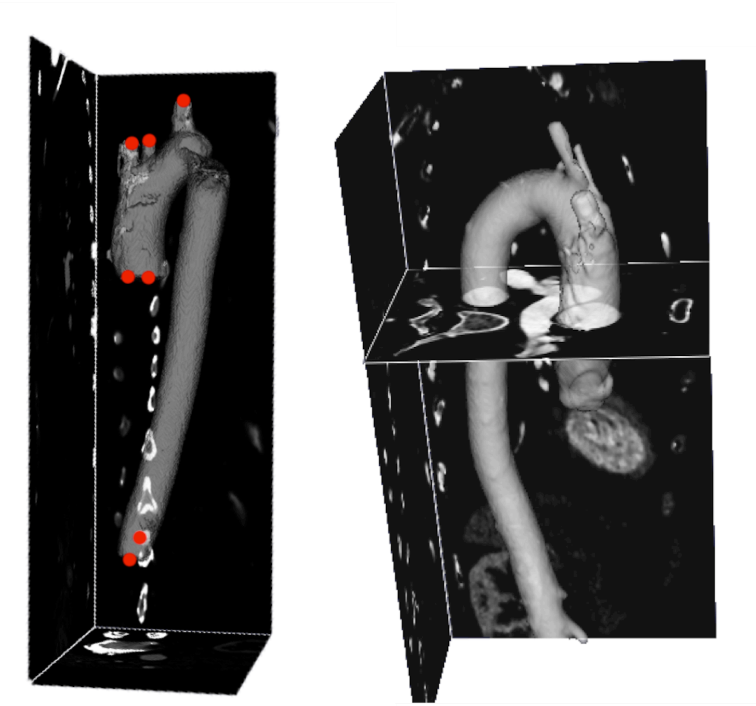

Automatic segmentation of 4D CTA[trentin2015]**:** shift

Hypothesis:

- two subsequent time instants do **not experience high changes** of position

Remark:

- the aortic arch level set produced is **a signed distance function**

Method:

- result of the evolution at 1st time instant is **shifted 1 mm inside** the vessel
- the shifted initialization is used as **initial level set** for the **subsequent time instant**

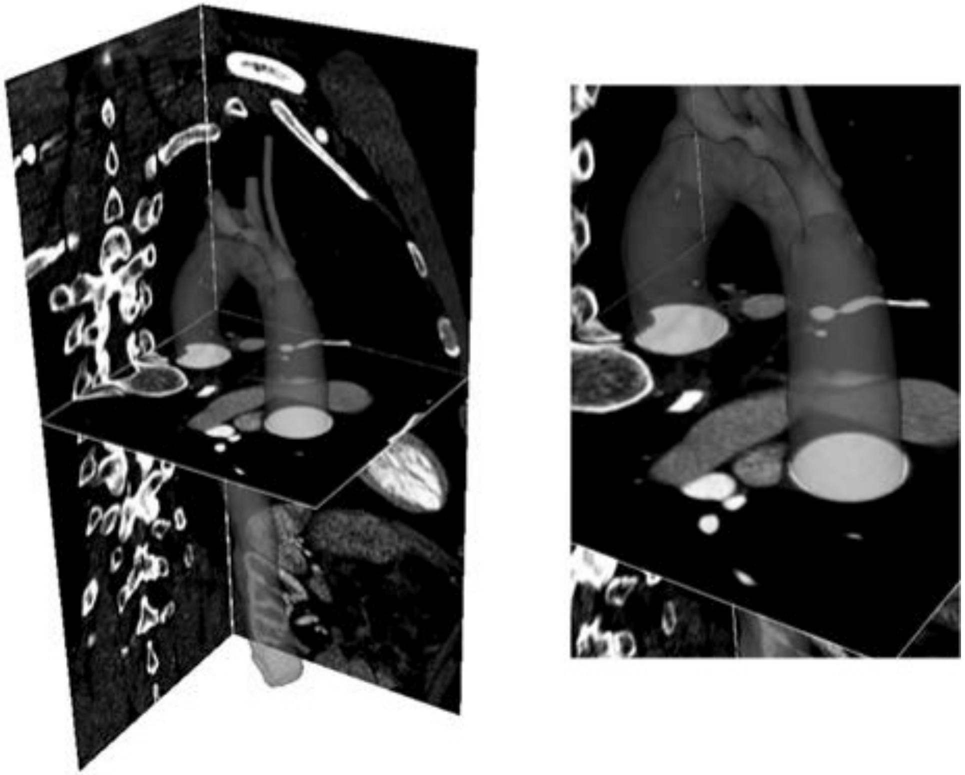

Result of the shift of 1 mm inside the vessel, displayed on the 4D CTA at the 1st time instant

Automatic segmentation of 4D CTA

Automatic segmentation of 4D CTA: new pipeline[trentin2015]

- equation is then evolved with parameters: $w_1 = 0.4$, $w_2 = 0.4$, and $w_3 = 1.0$
- **automatically** repeated for each time step
- user's workload **reduced**

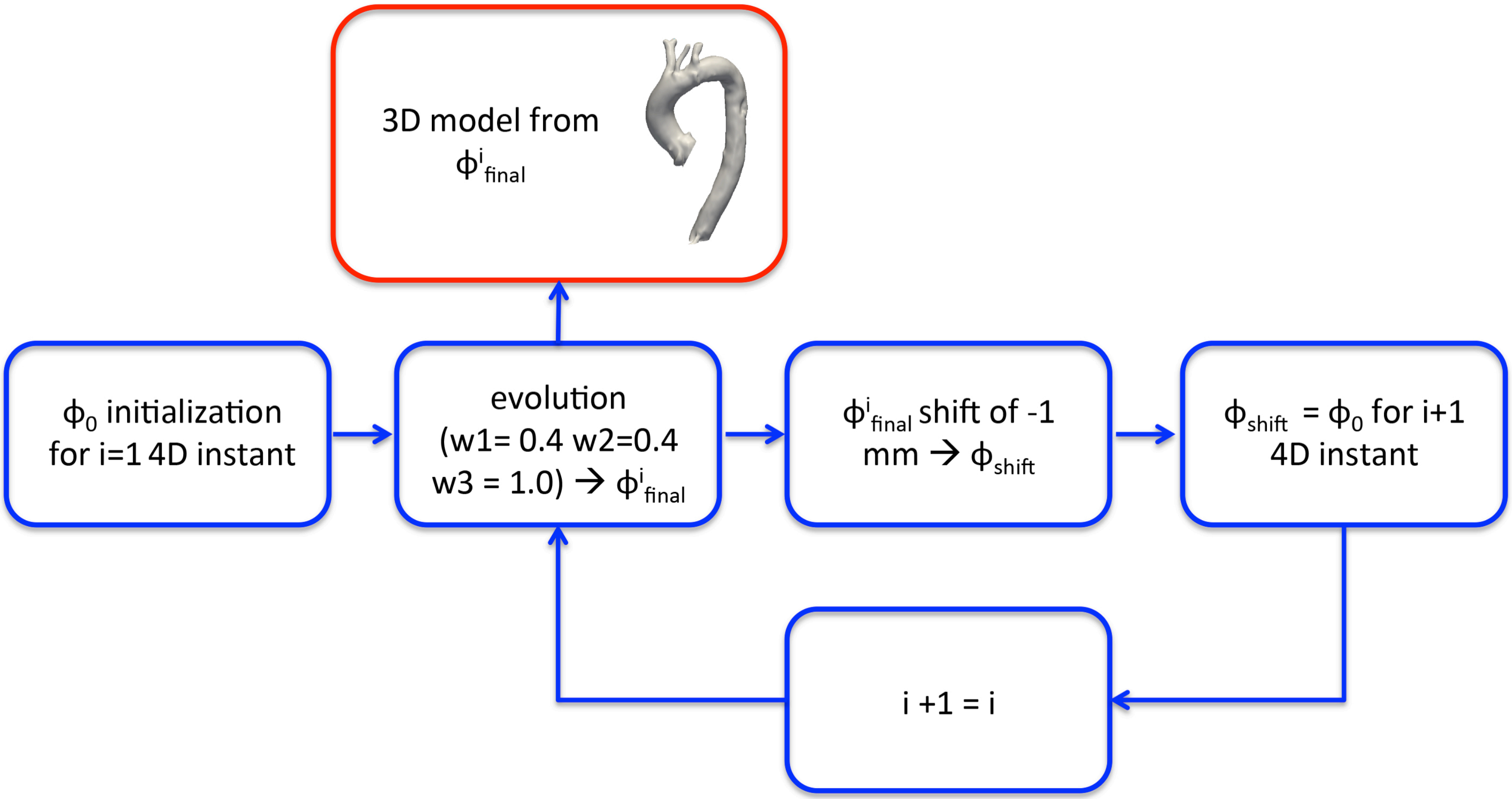

Centerline definition and branch splitting procedure

Centerline

- synthetic descriptor of vessel geometry drawn between an inflow section and multiple outflow sections
- locally **maximizes the distance** from the vessel's wall[antiga2008]

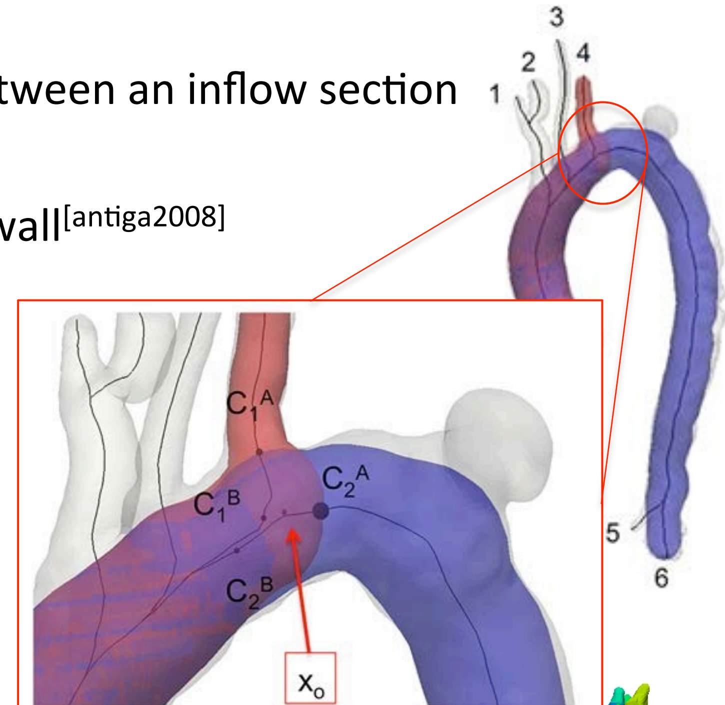

Bifurcation reference system (BRS) definition:

- **four points** delimit a segment on each centerline
- the segment identify the bifurcation region
- the four points identify the **origin of the bifurcation** region

Branch extraction procedure:

- BRS allows decomposition of centerlines in different tracts belonging to different branches
- each centerline $c_i(s)$ grouped into tracts defined by s in $[0,s_i^B]$ and $[s_i^A, L_i]$
- it is possible to **decompose R^3 into groups** exploiting a distance metrics
- the i^{th} group is composed by the union of points closer to group function $\gamma_i(s)$ than to any other group function $\gamma_j(s)$

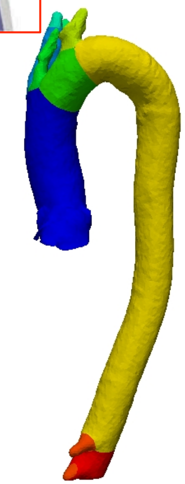

Pre- and Post-TEVAR surface registration

Bifurcation reference system transformation

- **compare** pre- and post-TEVAR 3D reconstructed models
- assess good outcomes
- **understand the changes** induced by the metallic stent-graft on vessel's shape
- **track changes** experienced by the thoracic aorta during the cardiac cycle

A rigid-body transformation between the models under investigation is needed

$$\mathbf{x}_{\mathbf{A}}^{\mathbf{transf}} = R_{AB}(\mathbf{x}_{\mathbf{A}}) + \mathbf{T}_{\mathbf{AB}}$$

where R_{AB} is a rotation matrix and a T_{AB} is a translation vector

We **choose** to:

- transforms not a set of point defined by the user but a reference system integral with the surfaces under investigation
- simple but robust

Bifurcation reference system transformation

Bifurcation reference system BRS is:

- **stable** than other points along the centerline

An alignment of the pre-TEVAR BSR into the post-TEVAR BSR is performed.

Translation vector $T_{PrePost}$:

- distance between the origin of the BSRs:

$$\mathbf{T_{PrePost}} = X[i]_{pre} - X[i]_{post}$$

Rotation matrix $R_{PrePost}$:

- build up from the rotation angles
- Euler angles - three angles to describe the orientation of a rigid body in 3-dimensional Euclidean space

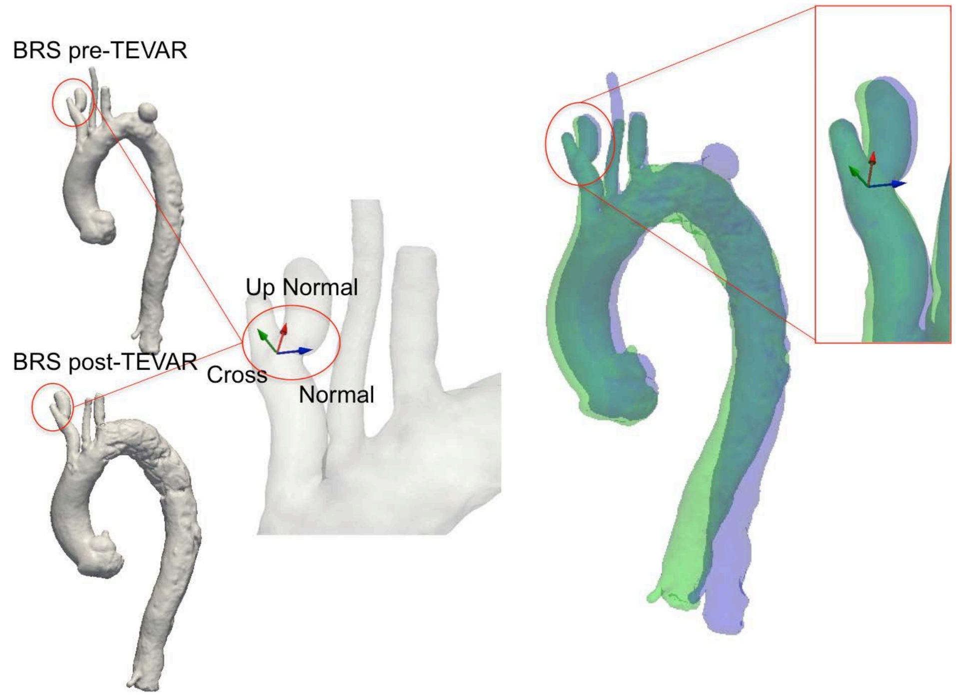

Bifurcation reference system transformation

The **three angles** are defined as follows:

- α is the angle between the Normalpre axis and the N axis
- β is the angle between the UpNormalpre axis and the UpNormalpost axis
- γ is the angle between the N axis and the Normalpost axis

$$R_{PrePost} = R_{UpNormal^{pre}}(\alpha)\, R_N(\beta)\, R_{UpNormal^{post}}(\gamma)$$

$$R_{UpNormal^{pre}}(\alpha) = \begin{pmatrix} \cos(\alpha) & -\sin(\alpha) & 0 \\ \sin(\alpha) & \cos(\alpha) & 0 \\ 0 & 0 & 1 \end{pmatrix}$$

$$R_N(\beta) = \begin{pmatrix} 1 & 0 & 0 \\ 0 & \cos(\beta) & -\sin(\beta) \\ 0 & \sin(\beta) & \cos(\beta) \end{pmatrix}$$

$$R_{UpNormal^{post}}(\gamma) = \begin{pmatrix} \cos(\gamma) & -\sin(\gamma) & 0 \\ \sin(\gamma) & \cos(\gamma) & 0 \\ 0 & 0 & 1 \end{pmatrix}$$

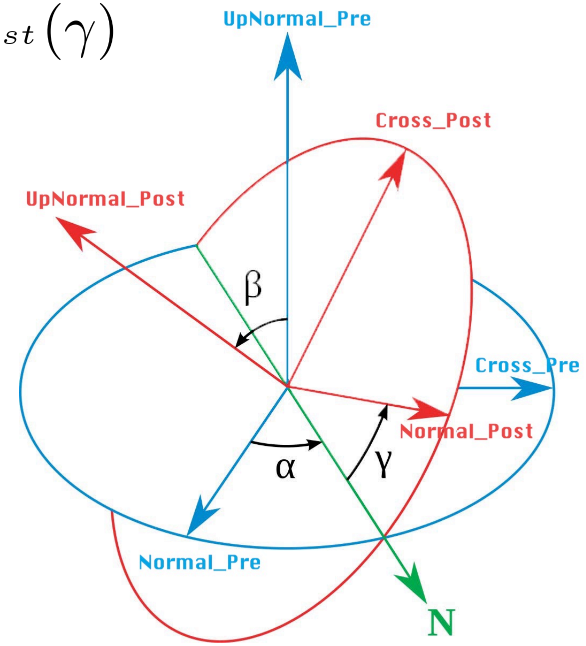

$$\mathbf{x}^{\mathbf{transf}}_{\mathbf{Pre}} = R_{PrePost}(\mathbf{x}_{\mathbf{Pre}}) + \mathbf{T}_{\mathbf{PrePost}}$$

Angular parametrization of vessel's surface is exploited to perform a surface data analysis → outer contour lines

Given a cylindrical surface $\partial\Gamma_i$ of a branch i with extremities given by two topological circle ψ_{i0} and ψ_{i1}, we search for a bijective mapping

$$\Phi : \partial\Gamma_{i_{\mathbf{x}}} \to \mathcal{U}_{\mathbf{u}}$$

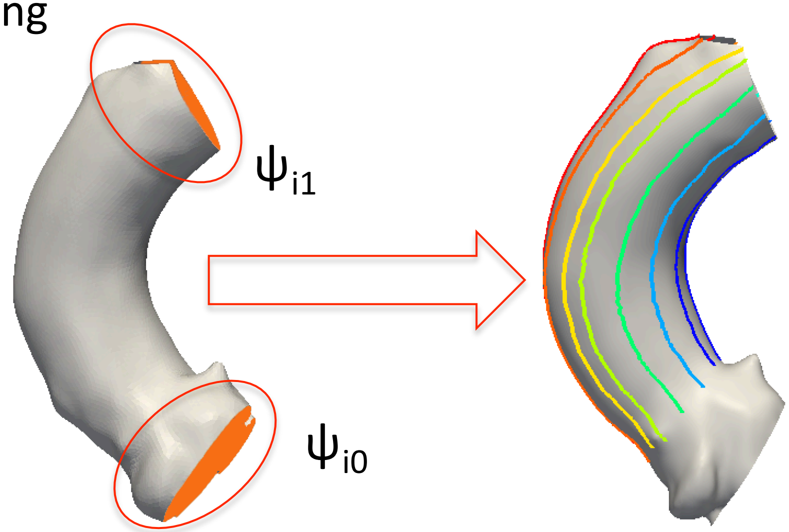

$\mathcal{U} \subset R^2$ → parametric space in the coordinates $\mathbf{u} = (u, v)$

- $u \in [0, L_i]$ → **the longitudinal parametric** coordinate
- $v \in [-\pi, \pi]$ → **the periodic circumferential parametric** coordinate
- $\Phi(\mathbf{x}) = (0, v)$ on ψ_{i0} and $\Phi(\mathbf{x}) = (L_i, v)$ on ψ_{i1}

Outer contour lines computation

Longitudinal mapping → computing a harmonic function with extremes on the branch boundaries

Computation of the harmonic function f = f(x), $x \in \partial\Gamma_i$ → performed by solving the partial differential equation:

$$\Delta_B f = 0$$

with f(x) = 0 on ψ_{i0}, f(x) = 1 on ψ_{i1} and Δ_B is the Laplace-Beltrami operator.

Circumferential mapping → angular position of surface points around the centerline, i.e., $[-\pi, \pi]$, determined by a set of normals n(s) along the curve

The parallel transport approach is exploit:

- frame (t(s+ds), n(s+ds), b(s+ds)) → derived from frame (t(s), n(s), b(s)) rotating t(s) into t(s+ds) around the vector $n_s = t_s \times t_{s+ds}$ in the osculating circle plane and than translated to (s+ds)
- frame rotated of a minimal quantities → no twist introduced

Outer contour lines computation

Given[Antiga2004]:

- s the curvilinear abscissa
- *n* the centerline normals,

We compute $v(\mathbf{x})$ for each point **x** ∈ Γ_i (surface under investigation) finding:

- its nearest point c(s) on the centerline
- the projection **x*** of **x** on the plane normal to t(s) and computing

$$v(\mathbf{x}) = \arccos((\mathbf{x}^* - c(s)) \cdot n(s))$$

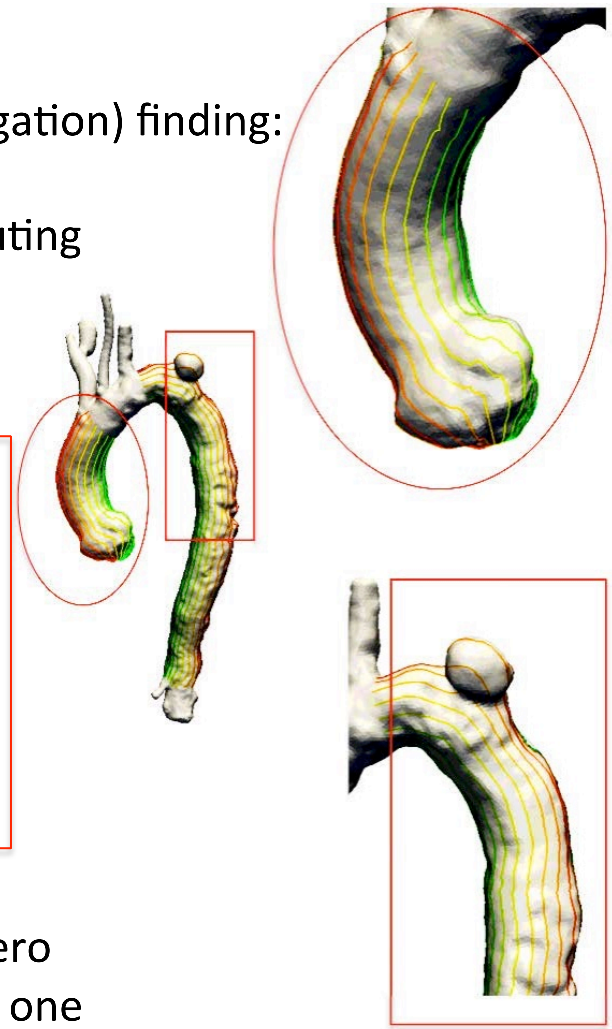

Decide to extract 10 iso-line with values in the interval I = [−π, −4/5π, −3/5π, −2/5π, −1/5π, 0, 1/5π, 2/5π, 3/5π, 4/5π, π] for each outer contour line we define the outer length OL as:

$$OL(\theta) = \int_{P_0(\theta)}^{P_1(\theta)} s\, ds \qquad \theta \in I$$

where s → the curvilinear abscissa

P_0 → initial point, the longitudinal parametric map has value zero

P_1 → the final point, the longitudinal parametric map has value one

Outer contour lines computation

Moreover we introduce a relative quantity to track the **changes in space** experienced by the aorta, named Outer Length Changes (OLC), expressed in percentage and defined as follows:

$$OLC = \frac{Amplitude(OL(\theta))}{A_{v_{space}}(OL(\theta))}$$

where

$$Amplitude(OL(\theta)) = (\max_{\theta \in I}(OL(\theta)) - \min_{\theta \in I}(OL(\theta)))$$

$$A_{v_{space}}(OL(\theta)) = \frac{1}{10} \sum_{\theta \in I} OL(\theta)$$

Clinical interpretation: high values of OLC may suggest high bending movements of the aorta

Levels of interest: tool defines automatically six levels of interest[trentin2015]

section A: level of the sino-tubular junction (STJ)

- **30 sections** cut the proximal aorta from the valvular plane upward (1mm spaced)
- local minima of the difference in area between the sections return the **STJ**

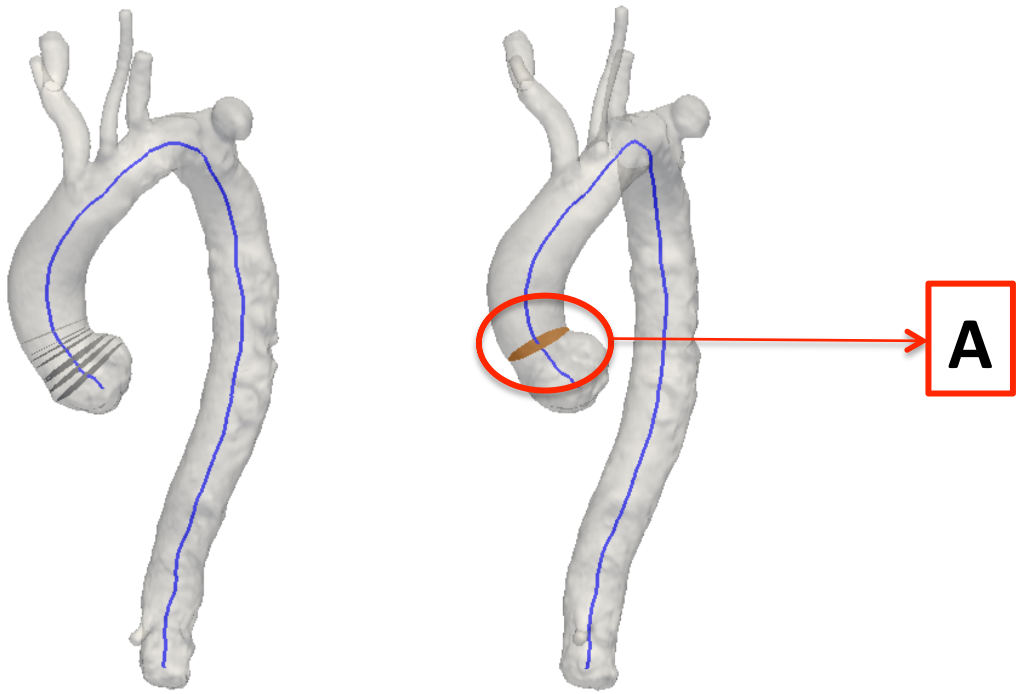

Levels of interest detection

Levels of interest: tool defines automatically six levels of interest

section B: 1 cm proximal to brachiocephalic trunk

- point where the centerlines referring to the ascending aorta and the innominate artery divide

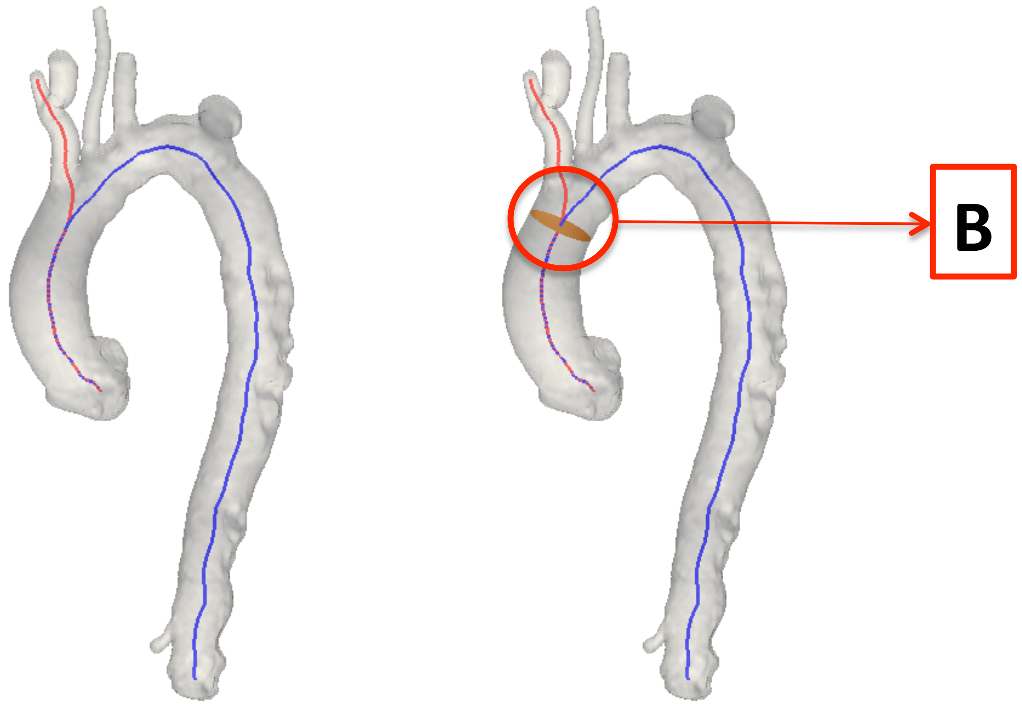

Levels of interest detection

Levels of interest: tool defines automatically six levels of interest

section C: left subclavian artery (LSA)

- point just after the LSA

section D: 10 cm distal to LSA

section E: 20 cm distal to LSA

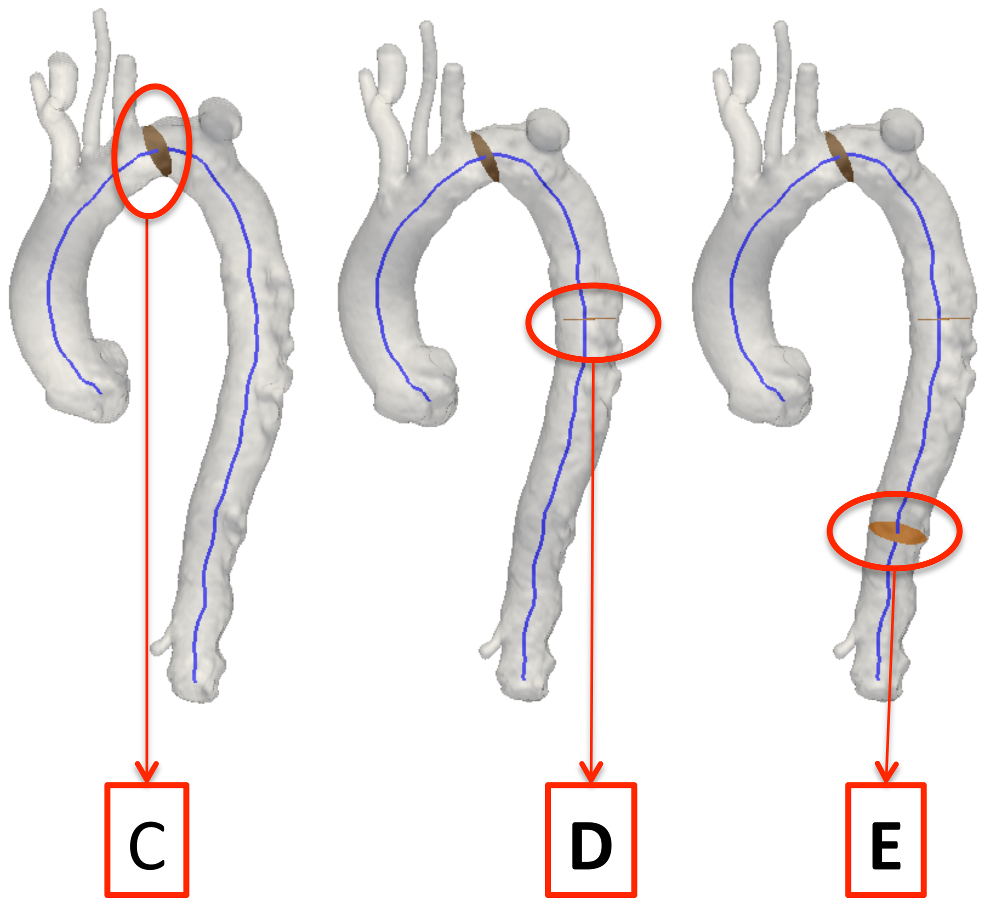

Levels of interest detection

Levels of interest: tool defines automatically six levels of interest

section F: level of celiac bifurcation

- point where the centerlines referring to the descending aorta and the celiac artery divide

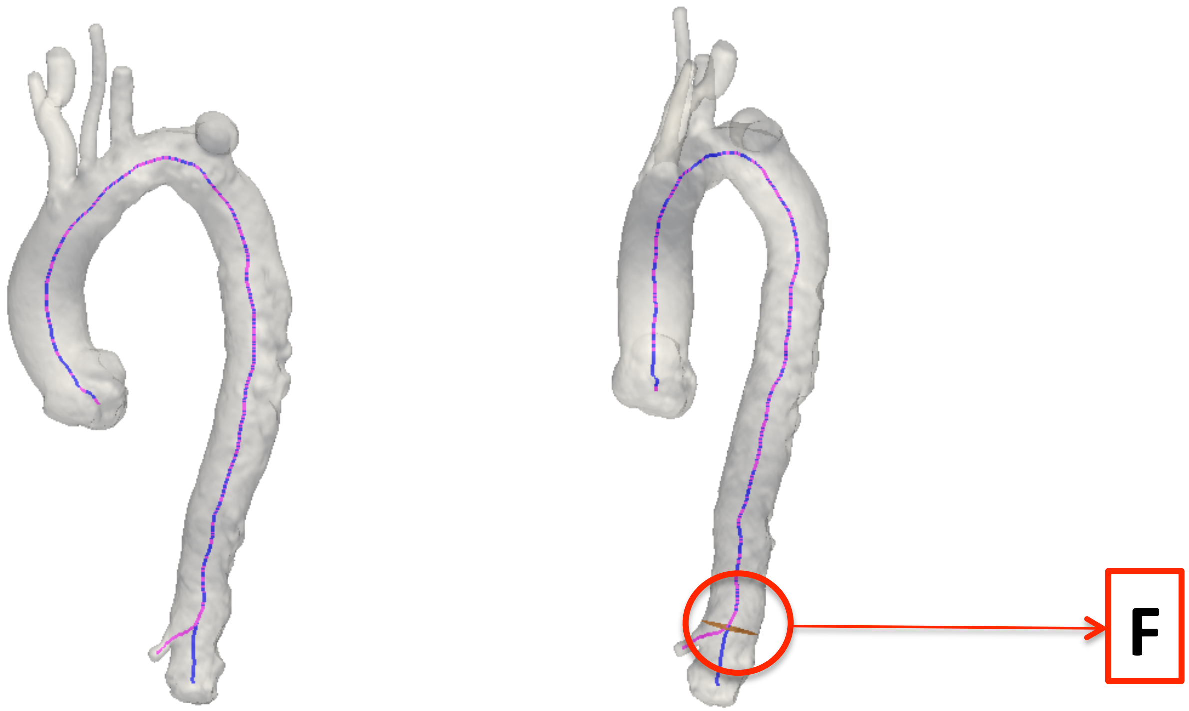

Measurements → for each level of interest

AREA → triangulation of the section of interest and sum the area of each triangle over the entire section

DIAMETER MINIMUM

$$d_{min}(S) = \min_{\mathbf{x}\in\partial S}\left(\max_{\mathbf{y}\in\partial S}\left(dist(\mathbf{x},\mathbf{y})\right)\right)$$

DIAMETER MAXIMUM

$$d_{max}(S) = \max_{\mathbf{x}\in\partial S}\left(\max_{\mathbf{y}\in\partial S}\left(dist(\mathbf{x},\mathbf{y})\right)\right)$$

where **x** and **y** are coordinates of the points of the contour ∂S of the section S, and dist(·) is the Euclidean distance

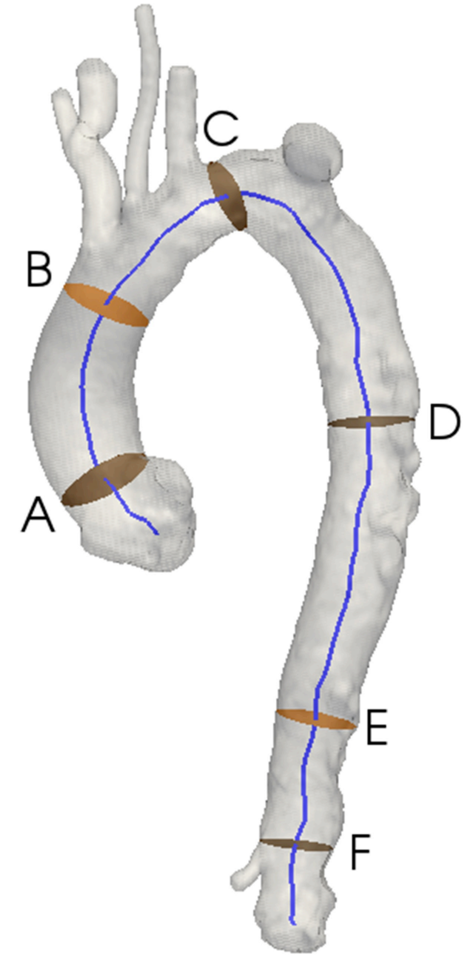

Measures → for each level of interest

LENGTH → L1, L2 and L3 of aortic arch between A and B, B and C, C and F

TOTAL LENGTH → L of the thoracic aortic arch from section A to section F

$$l(S_1, S_2) = \int_{S_1}^{S_2} s\, ds$$

where s is the curvilinear abscissa defined on the centerline and s_1 and s_2 are the points of the centerline on the generic sections S_1 and S_2

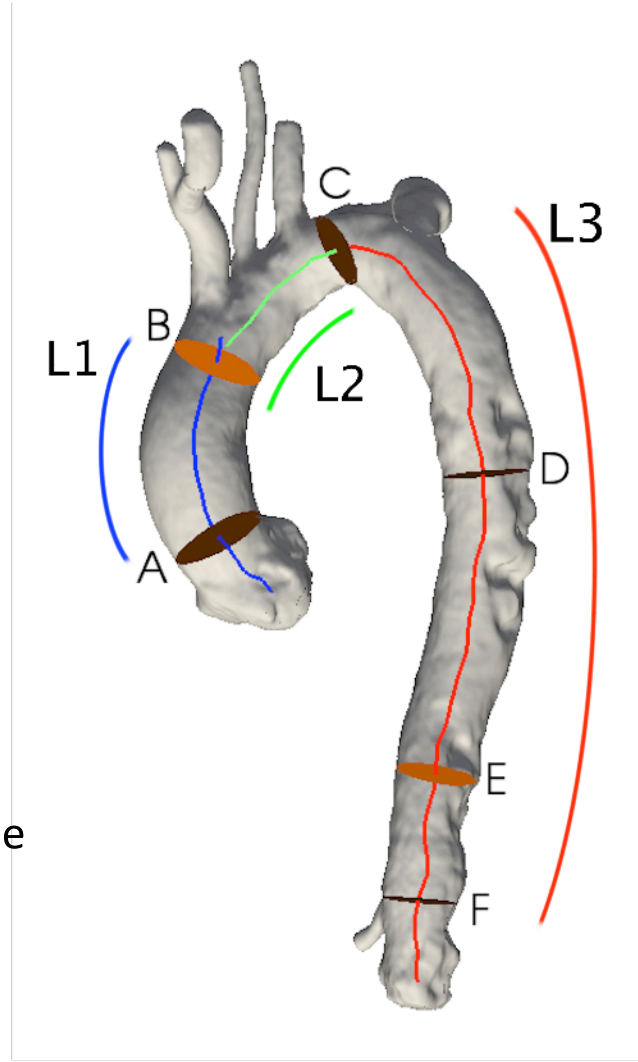

Measurements in time → relative measurements

Area Changes: AC

$$AC = \frac{Amplitude(Area)}{A_{v_{time}}(Area)}$$

Diameter Changes: DC

$$DC = \frac{\frac{1}{2}(Amplitude(d_{min}) + Amplitude(d_{max}))}{\frac{1}{2}(A_{v_{time}}(d_{min}) + A_{v_{time}}(d_{max}))}$$

Length Changes: LC

$$LC = \frac{Amplitude(l)}{A_{v_{time}}(l)}$$

Mean Shape: MS

$$MS = \frac{A_{v_{time}}(d_{min}(S))}{A_{v_{time}}(d_{max}(S))}$$

where

$$Amplitude(\mathbf{X}) = (\max_{i \in time}(\mathbf{X}[i]) - \min_{i \in time}(\mathbf{X}[i]))$$

$$A_{v_{time}}(\mathbf{X}) = \frac{1}{8}\sum_{i=1}^{8}\mathbf{X}[i]$$

with **X** vector containing quantities' values for each time instant

Clinical interpretation: measurements changes suggest high deformation in time

Results: the TAA dataset

Results: the dataset → 8 patients with TAA

6 male and 2 female, mean age 71

Patient	Sex	Age	Diagnosis	stent-graft type	Size graft 1	Size graft 2	Size Graft 3
1	m	79	TAA	Relay, Bolton	42-42-100	38-38-100	
2	m	65	TAA	Relay, Bolton	38-38-100		
3	m	61	TAA	Valiant, Medtronic	38-38-125	40-40-150	44-44-150
4	m	80	TAA	Valiant, Medtronic	36-36-100	38-38-100	
5	m	70	TAA	Valiant, Medtronic	36-36-100		
6	m	75	TAA	Valiant, Medtronic	42-42-150		
7	f	77	TAA	Valiant, Medtronic	38-38-200	38-38-200	
8	f	59	PAU/TAA	Relay, Bolton	34-34-100		

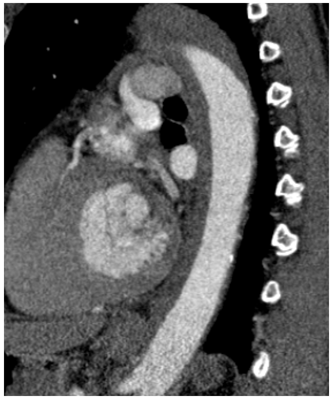

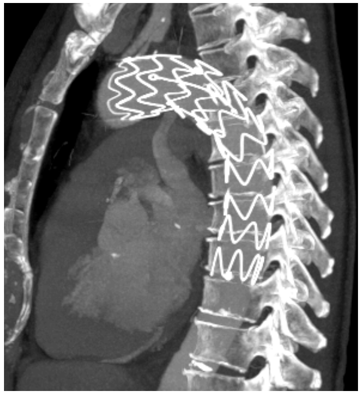
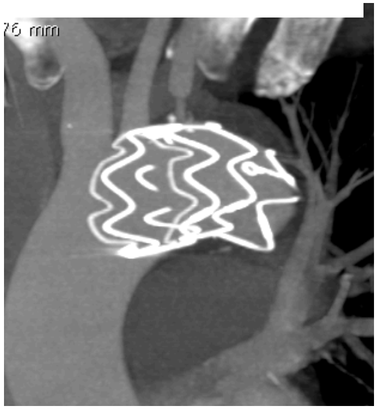

G. B., F. N., **Chiara Trentin**, M. C., F. A., F. M., J. H., *"Impact of Thoracic Endovascular Repair on Aortic Strain in Patients with Aneurysm"*, under submission.

Results: the TAA dataset

Length changes

- Patient 1
  - 4.9% → 6.4% in L2
  - 3.9% → 3.9% in L3
- Patient 2
  - 5.6% → 7.8% in L1
  - 6.8% → 9% in L2
  - 4.8% → 3.8% in L3
- Patient 3
  - 6.6% → 8.5% in L2
  - 5.6% → 3% in L3
- Patient 4
  - No post-TEVAR data

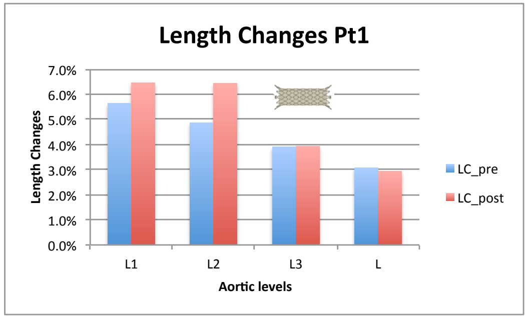

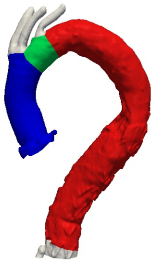

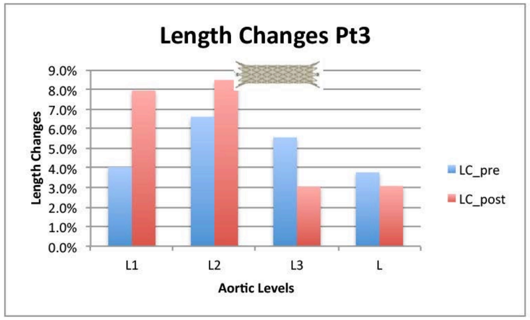

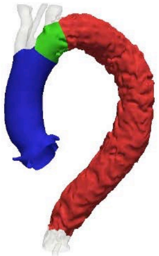

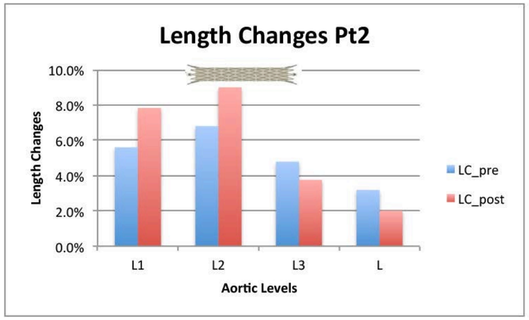

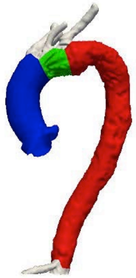

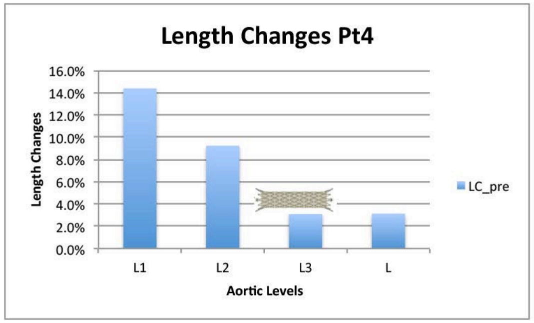

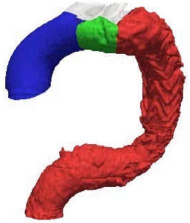

Results: the TAA dataset

- Patient 5
  - 4.9% → 4.8% in L2
  - 2.3% → 1.4% in L3
- Patient 6
  - 4.3% → 5.9% in L1
  - 6% → 6.7% in L2
  - 1.4% → 3.7% in L3
- Patient 7
  - 4.7% → 5.2% in L2
  - 1.2% → 8% in L3
- Patient 8
  - 5.6% → 15.6% in L1
  - 9.5% → 8.8% in L2
  - 2.5% → 5.4% in L3

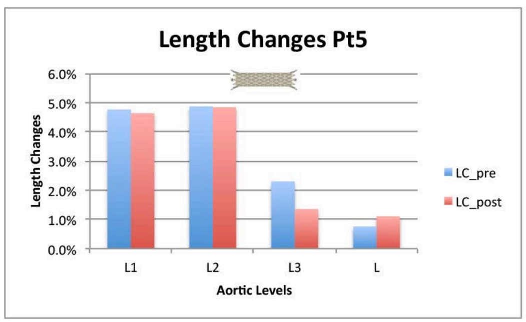

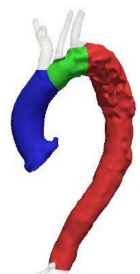

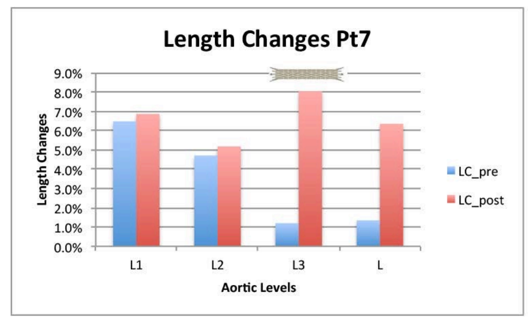

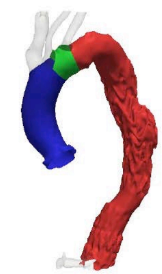

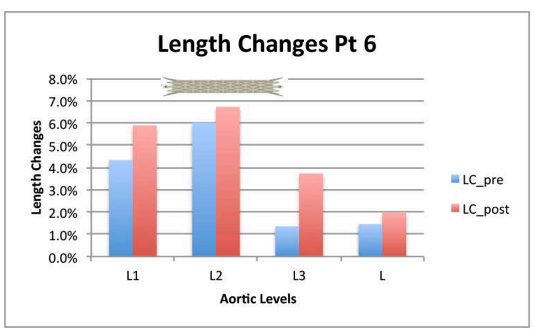

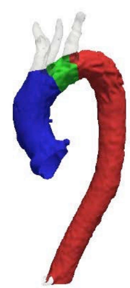

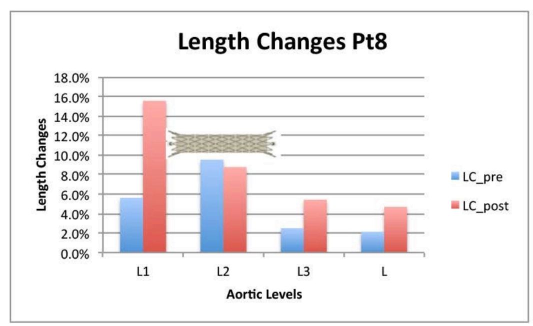

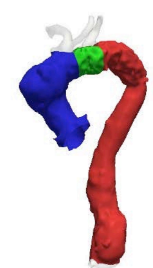

Results: the TAA dataset

Outer length changes OLC

- overall outer length changes, **tracked in space** not in time over the entire hearth cycle
- OLC is **double in values** in the ascending aorta with respect to the descending aorta
- OLC in the ascending aorta shows a **pressure like shape**
- OLC in the descending aorta is **slightly lower** post-TEVAR

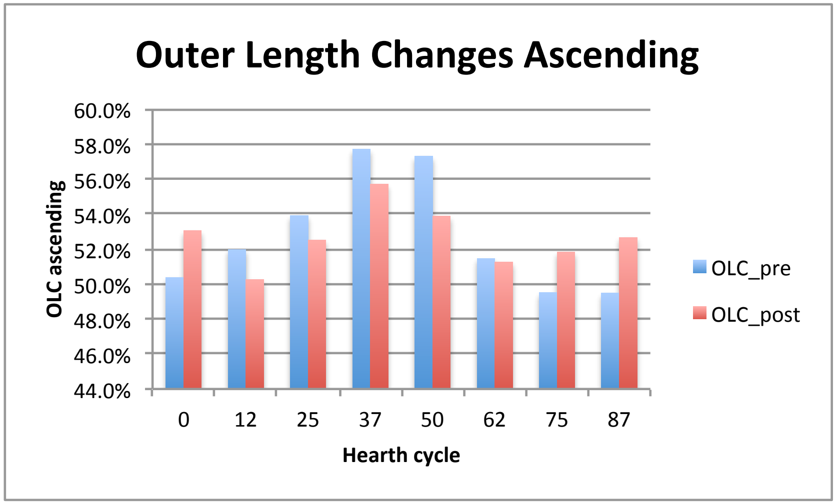

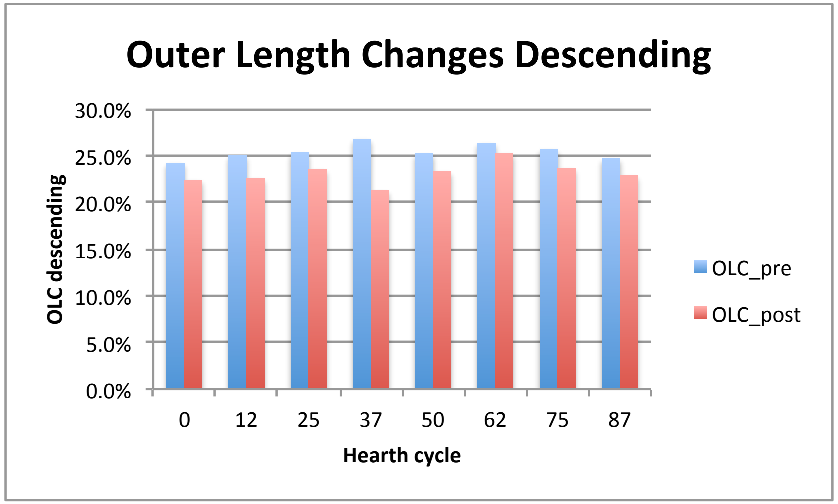

Results: the TBAD dataset

Results: the dataset → 2 patients with TBAD and 1 control

Patient 1

- 53-year old female with acute TBAD

Patient 2

- 55- year old male with Marfan syndrome and ruptured acute TBAD

Patient 3

- Healthy control patient: 49-year old female with thoracic pain, no vascular pathology on CT

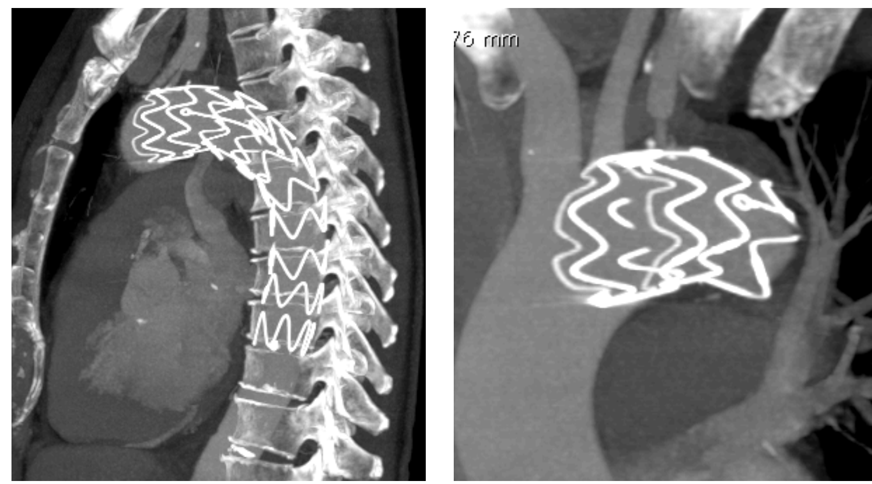

Trentin, Chiara, F. E., C. M.,A. F., "An automatic tool for thoracic aorta segmentation and 3D geometric analysis," in *Image and Signal Processing and Analysis (ISPA), 2015 9th International Symposium on* , pp.60-65, 7-9 Sept. 2015

Results: the TBAD dataset

- Length changes of L, L1, L2, and L3
- comparison with the healthy control
- Length Changes in L2: from 8.2% (before TEVAR) to 13.1% (after TEVAR)
- region of **increase located just before stent-graft**

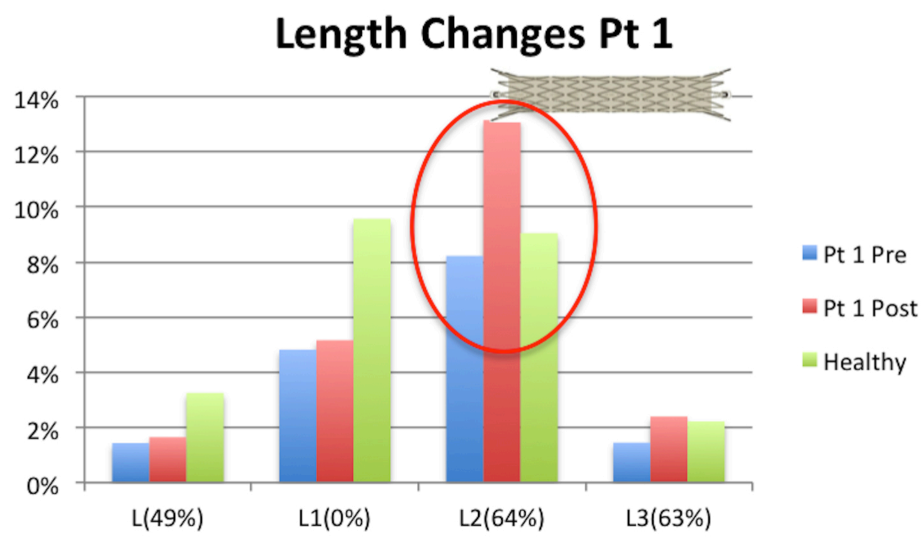

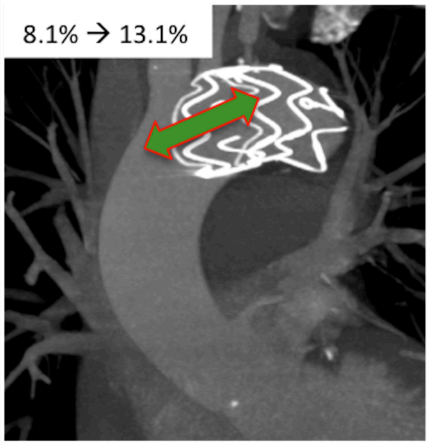

Results: the TBAD dataset

- Length changes of L, L1, L2, and L3
- comparison with the healthy control
- Length Changes in L1: from 9.4% (before TEVAR) to 15.8% (after TEVAR)
- Length Changes in L3: from 4.8% (before TEVAR) to 1.6% (after TEVAR)
- **increase before** stent-graft, **contraction at** the stent-graft

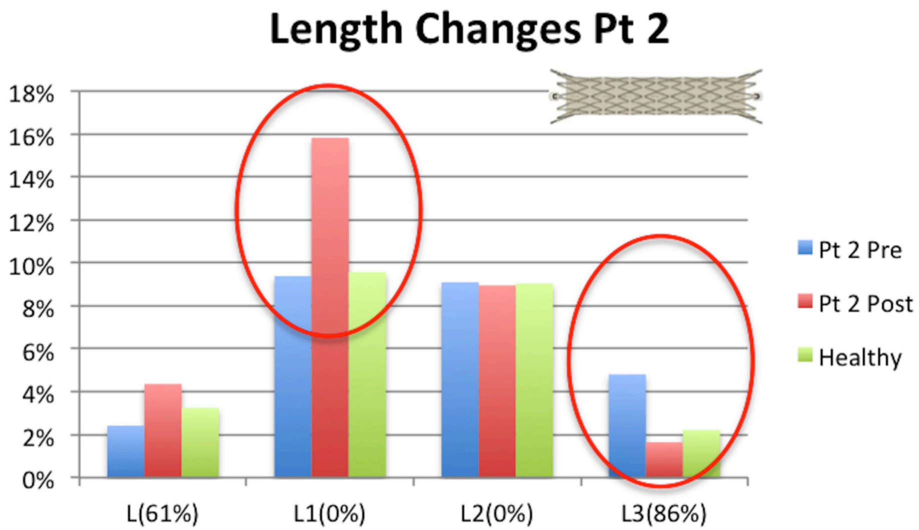

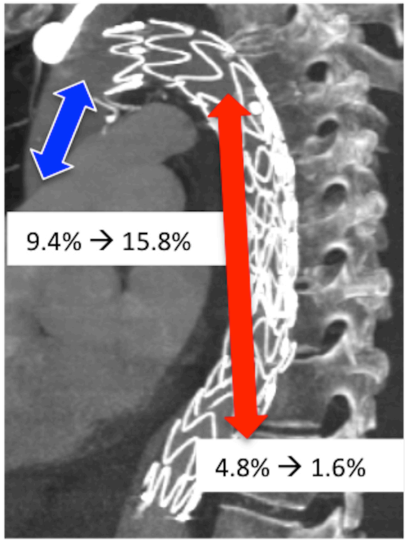

Results: the TBAD dataset

Outer length changes OLC

- overall outer length changes, **tracked in space** not in time over the entire hearth cycle
- OLC is **double in values** in the ascending aorta with respect to the descending aorta
- OLC in the ascending shows **a pressure like pattern in the pathologic** patients and a more **casual pattern for the healthy control**
- OLC in the descending aorta is **slightly lower** post-TEVAR
- OLC in the descending aorta for the healthy control is **higher in value overall**

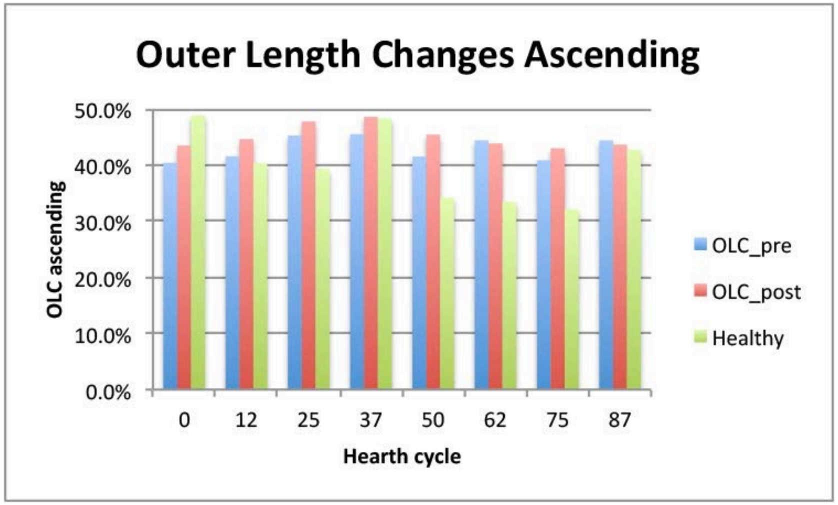

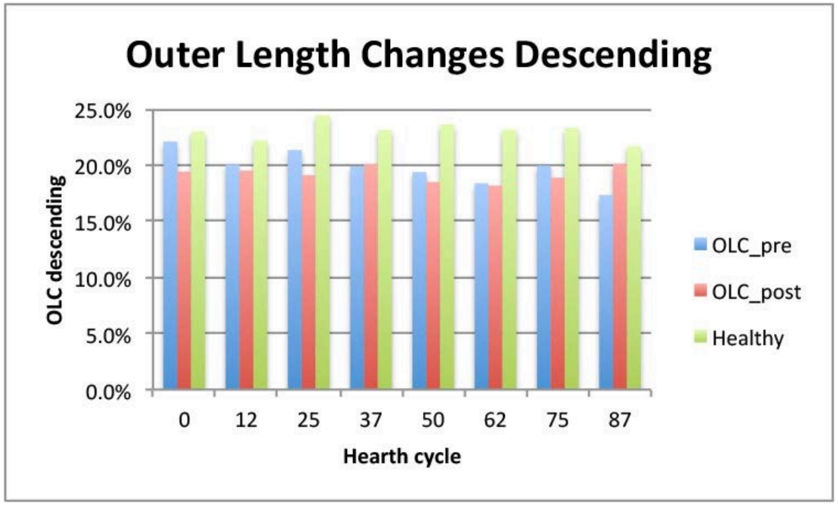

Conclusions

- **automatic** tool to segment thoracic aorta from 4D CTA images
- automatic **detection of levels of interest**
- automatic **geometric feature computation**
- **track** the dynamic changes of the thoracic aorta
- **expand** the knowledge of stent-graft behaviour
- actually used by the **University Medical Centre Utrecht**

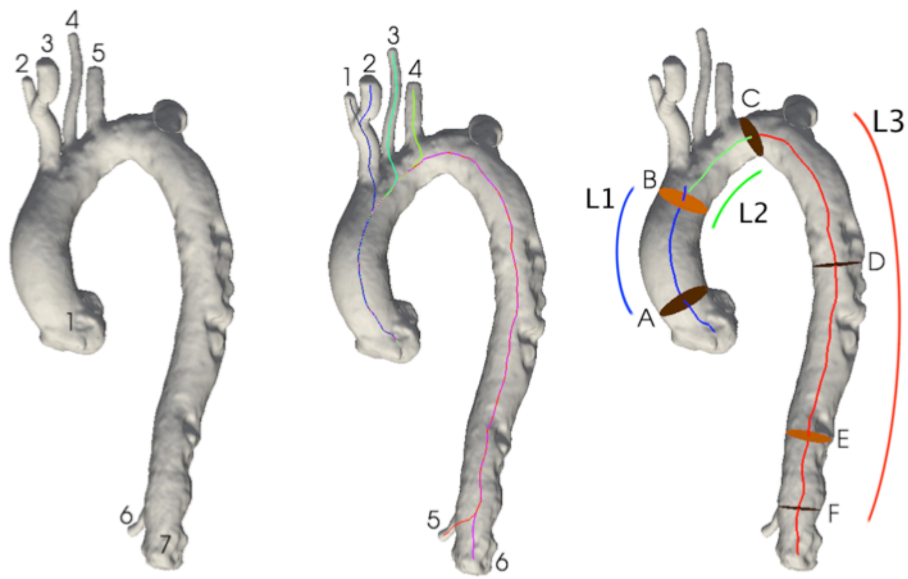

Future work

- image quality and artefacts **avoidance**
- image **registration**
- **fully integration** of the steps composing the tool (set of libraries)
- measurements of **torsion and tortuosity** need to be included as well as a method for centerline resampling (spline)
- integration of a **statistical analysis**

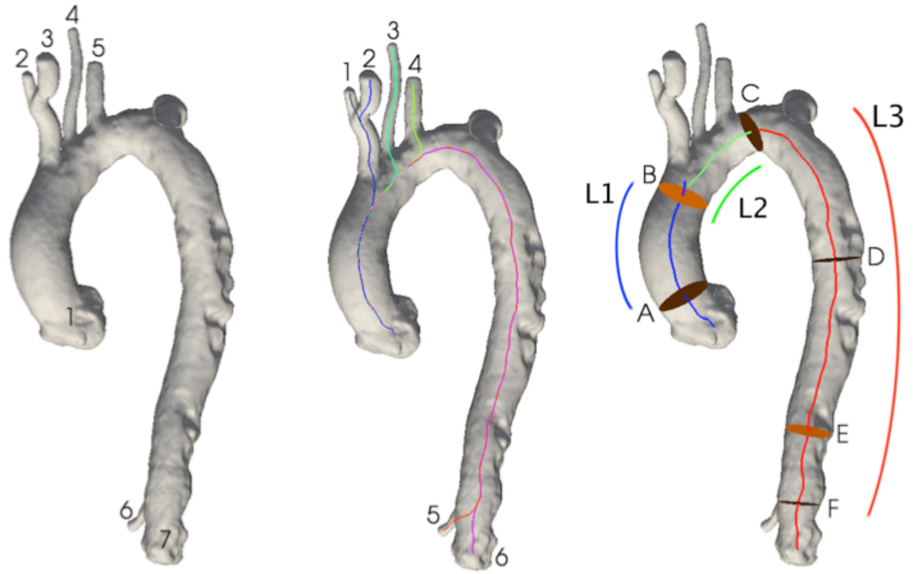

Thank you!

References

[vanP2009] van Prehn J, Bartels LW, Mestres G, Vincken KL, Prokop M, Verhagen HJ, Moll FL, van Herwaarden JA. Dynamic aortic changes in patients with thoracic aortic aneurysms evaluated with electrocardiography- triggered computed tomographic angiography before and after thoracic endovascular aneurysm repair: Preliminary results. . Ann Vasc Surg. 2009; 23:291-297.

[muhs2006] Muhs BE, Vincken KL, van Prehn J, Stone MK, Bartels LW, Prokop M, Moll FL, Verhagen HJ. Dynamic cine-CT angiography for the evaluation of the thoracic aorta; insight in dynamic changes with implications for thoracic endograft treatment. Eur J Vasc Endovasc Surg. 2006; 32:532- 536.

[vanK2009] van Keulen JW, van Prehn J, Prokop M, Moll FL, van Herwaarden JA. Dynamics of the aorta before and after endovascular aneurysm repair: A systematic review. Eur J Vasc Endovasc Surg. 2009; 38:586-596.

[piccinelli2009] Piccinelli M, Veneziani A, Steinman DA, Remuzzi A, Antiga L. A framework for geometric analysis of vascular structures: Application to cerebral aneurysms. IEEE Trans Med imaging. 2009; 28:1141-1155.

[antiga2008] Antiga, Luca, et al. An image-based modeling framework for patient- specific computational hemodynamics. Medical & biological engineering & computing, 2008, 46.11: 1097-1112.

[trentin2015] Trentin, Chiara; Faggiano, Elena; Conti, Michele; Auricchio, Ferdinando, "An automatic tool for thoracic aorta segmentation and 3D geometric analysis," in Image and Signal Processing and Analysis (ISPA), 2015 9th International Symposium on , pp.60-65, 7-9 Sept. 2015